Progress In Electromagnetics Research C, Vol. 31, 17–28, 2012

DESIGN OF COMPACT DUAL-BAND BANDPASS FILTER USING $\lambda/4$ BENDED SIRS

L. Lu*, **M. Z. Zhu, F. Gao, and X. L. Liu**

National Key Laboratory of Antennas and Microwave Technology, Xidian University, Xi'an, Shaanxi 710071, China

Abstract—A simple method and structure to design a dual-band filter by using $\lambda/4$ stepped impedance resonators (SIRs) is presented in this paper. This filter has enhanced performance, including a good rolloff in the stopband and good insertion-loss response. The structure is compact and easy to fabricate. The circuit is investigated with the even-odd mode theory to prove the existence of transmission zeros. The dual-band response is analyzed by using SIR theory and the parallel-coupled line theory. Based on the proposed filter topology, two dual-band filters center operating frequency at 2.4 GHz and 5.2 GHz respectively with different configurations have been designed and one of them was tested, which validates the diversity of the filter configuration. Experimental results show that the measured and simulated performances are in good agreement. The overall area of the fabricated filter is $12\,\text{mm} * 12\,\text{mm}$.

1. INTRODUCTION

As known to all, communication technologies have been developing so fast that the demand of filters with two operating frequencies increases dramatically, and various dual-band filters have been extensively exploited and applied [1–13]. A good design of dual-band filter with planar structure should have advantages of compact size and steep selectivity for both bands. There are many methods to design a dual-band filter like combining two single-band filters which operate at different frequencies [1, 2], cascading a dual-band filter and a bandstop filter [3]. However, these methods would not effectively reduce the size and cost. Recently, more and more filters have been designed with stepped impedance resonators (SIRs) [5–13] due to the advantages of

Received 27 March 2012, Accepted 27 June 2012, Scheduled 3 July 2012

* Corresponding author: Lu Lu (lulu0925@163.com).

size compactness to the flexibility in controlling the ratio of the first and the second resonance frequencies. However, the dimensions of previous works are still large because the SIRs are arranged by the electrical coupling on the substrate. Therefore, the task of designing a dual-band bandpass filter (BPF) with compact size and good performance is still a challenge.

In this paper, a miniaturized dual-band filter using SIRs is proposed. An analysis of the generation of transmission zeros near the passband is made in Section 2 by using the even-odd mode theory. The filter design is described in Section 3, where the experimental example of the second-order SIR filter is designed. Since the filter has a better diversity in circuit layout which can be bended in more different styles, another filter with different configuration is shown. The simulated and measured results of the filter are shown in Section 4. Finally, a conclusion is given is Section 5.

2. ANALYSIS OF THE TRANSMISSION ZEROS

In Figure 1 is a filter centered at 2.4 GHz which is composed of two parallel-coupled (input and output) lines and two $\lambda/4$ resonators with sinuous configuration shaped as the letter "S" in order to reduce the size of the filter. The two SIRs are connected to each other by a via hole shorting to the ground. In this structure, electrical coupling is adopted since two ends of the resonators shorting to the ground are bent into parallel.

Shown in Figure 2 is an equivalent transmission line model of the structure in Figure 1. Since the structure is symmetric with respect to S, the even- and odd-mode theory may be applied to analyze this filter [4].

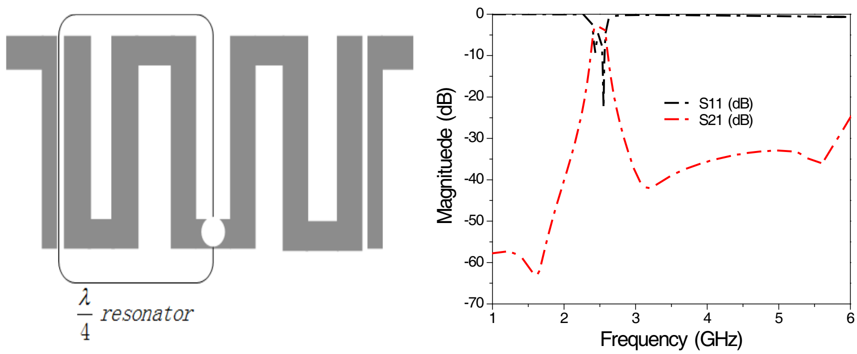

Figure 1. Configurations of the single-band filter and its simulated response.

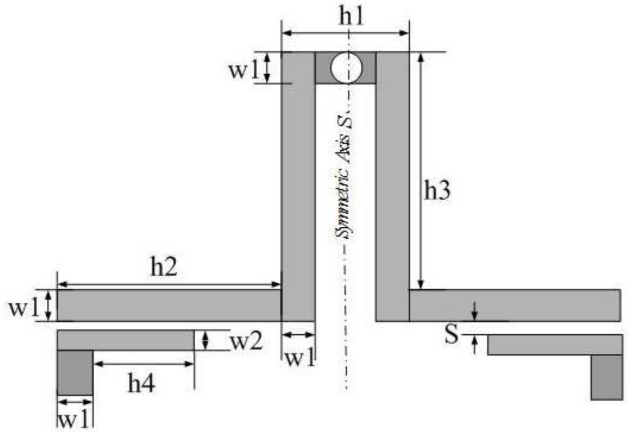

Figure 2. Equivalent transmission line model of the filter.

For the even-mode equivalent circuit in Figure 3(a), which has a short-ended coupling stub of impedance Z_{oe}, it's input impedance can be formulated as

$$Z^e_{\text{in}\cdot U} = jZ_{oe}\tan(\theta_{0e}) \tag{1}$$

$$Z^e_{\text{in}L} = Z_o\frac{Z^e_{\text{in}U} + Z_o\tan(\theta_2)}{Z_o + jZ^e_{\text{in}U}\tan(\theta_2)} \tag{2}$$

where Z_{oe} is the characteristic impedance excited at even mode. θ_{oe} is the electric length excited at even mode.

As presented in [5], the characteristic modes are named c mode and π mode in an asymmetric coupled line can be adopted. The even-mode impedance matrix $[Z^e_L]$ of pair L (with the condition $I2 = 0$; $I4 = 0$) is found as:

$$Z^e_{11V} = j\frac{R_c Z_{c1}\cot(\theta_c)}{R_\pi\left(1-\frac{R_c}{R_\pi}\right)} + j\frac{R_\pi Z_{c1}\cot(\theta_\pi)}{R_c\left(1-\frac{R_\pi}{R_c}\right)} \tag{3}$$

$$Z^e_{33v} = -j\frac{Z_{c2}\cot(\theta_c)}{1-\frac{R_c}{R_\pi}} - j\frac{Z_{\pi2}\cot(\theta_\pi)}{1-\frac{R_\pi}{R_c}} \tag{4}$$

$$Z^e_{13V} = Z^e_{31V} = -j\frac{R_c Z_{c2}}{\left(1-\frac{R_c}{R_\pi}\right)\sin(\theta_c)} - j\frac{R_\pi Z_{\pi2}}{\left(1-\frac{R_\pi}{R_c}\right)\sin(\theta_\pi)} \tag{5}$$

$$Z^e_{\text{in}V} = Z^e_{11V} + \frac{Z^e_{12V}Z^e_{21V}}{Z^e_{\text{in}L} - Z^e_{22V}} \tag{6}$$

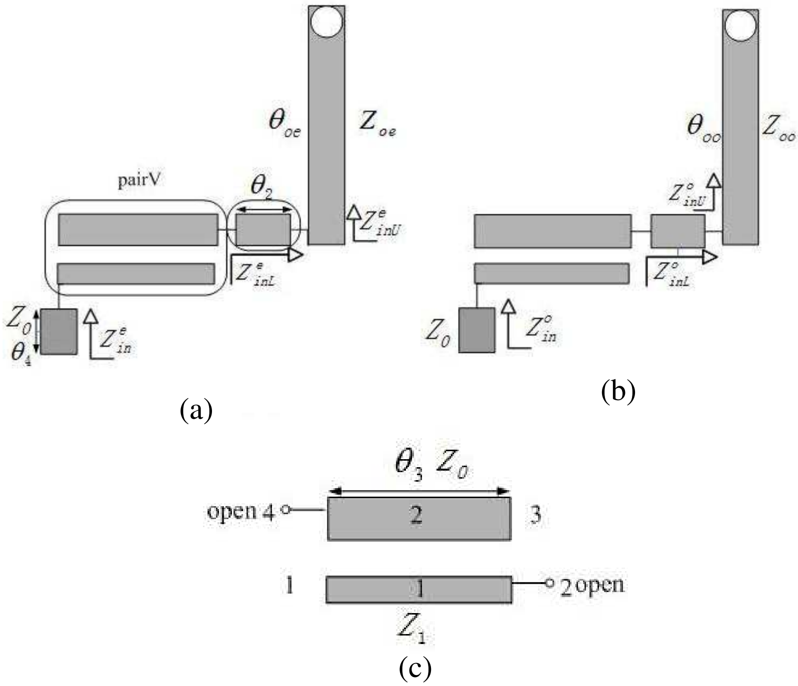

Figure 3. Even and odd-mode equivalent circuits of the proposed filter. (a) Even-mode and, (b) odd-mode, (c) pair V.

where R_c and R_π are the c mode and π mode voltage ratios; θ_c and θ_π are the c mode and π mode electric lengths; Z_{c1}, Z_{c2}, $Z_{\pi 1}$, and $Z_{\pi 2}$ are the c mode and π mode characteristic impedances.

Thus, the one-port input impedance

$$Z^e_{\text{in}} = Z_o \frac{Z^e_{\text{in}V} + Z_o \tan(\theta_4)}{Z_o + jZ^e_{\text{in}V} \tan(\theta_4)} \tag{7}$$

The even-mode input admittance can be attained as

$$Y^e_{\text{in}} = \frac{1}{Z^e_{\text{in}}} \tag{8}$$

By using the same procedure mentioned above, the odd-mode input admittance Y^o_{in} can be obtained by setting the short-circuited condition on axis S. The admittance matrix of the filter can be expressed in terms of Y^e_{in} and Y^o_{in} as

$$[Y] = \begin{bmatrix} Y_{11} & Y_{12} \\ Y_{21} & Y_{22} \end{bmatrix} = \begin{bmatrix} \frac{Y^e_{\text{in}}+Y^o_{\text{in}}}{2} & \frac{Y^e_{\text{in}}-Y^o_{\text{in}}}{2} \\ \frac{Y^e_{\text{in}}-Y^o_{\text{in}}}{2} & \frac{Y^e_{\text{in}}+Y^o_{\text{in}}}{2} \end{bmatrix} \tag{9}$$

With the derived admittances, one may solve the condition for the transmission zeros by equating Y_{in}^e and Y_{in}^o to obtain the transmission zeros from the equation $Y_{12} = 1/2(Y_{\text{in}}^e - Y_{\text{in}}^o) = 0$

As for an example of the filter with the dimensions of $w1 = 1\,\text{m}$, $w2 = 0.5\,\text{mm}$, $h1 = 3.5\,\text{mm}$, $h2 = 10\,\text{mm}$, $h3 = 12\,\text{mm}$, $h4 = 5\,\text{mm}$, $S = 0.3\,\text{mm}$ on the substrate with dielectric constant $\varepsilon_\gamma = 2.55$, loss tangent $\delta = 0.0029$, and thickness $h = 0.8\,\text{mm}$, the relation of Y_{21} is obtained as shown in Figure 4 with the formulas mentioned above. As shown in Figure 4, the transmission zeros appear at 1 GHz, 4.2 GHz and 5.7 GHz respectively.

3. DESIGN OF THE DUAL-BAND SIRS FILTER

In Section 2, we have used the even-odd mode theory to analyze transmission zeros. In this section, we use the coupling coefficient method to determine the circuit dimensions. The procedures are outlined below.

(1) Select a low-pass prototype with order N, we then have prototype elements g_i, with $i = 0, \ldots, N+1$. The fractional bandwidth is defined as $B = \Delta/f_o$, where Δ is the bandwidth of passband and f_o is the central frequency of passband. A dual-band filter at 2.4 GHz with 8% fractional bandwidth was designed. Its circuit is derived from the second-order prototype ($N = 2$) with $g_0 = 1.0000$, $g_1 = 0.8430$, $g_2 = 0.6220$, $g_3 = 1.3554$.

(2) Calculate the input and output external quality factor Q_{e1}, Q_{eN} and inter-coupling coefficients between two resonators

$$Q_{e1} = \frac{g_0 g_1}{B} \tag{10}$$

$$Q_{eN} = \frac{g_N g_{N+1}}{B} \tag{11}$$

$$M_{i,i+1} = \frac{B}{\sqrt{g_i g_{i+1}}}, \quad i = 1, 2, \ldots, N-1. \tag{12}$$

For the second-order filter ($N = 2$), $Q_{e1} = 10.54$, $Q_{\text{e}2} = 10.54$ and $M_{12} = 0.11$.

(3) Determine line impedance of the SIRs, the spacing between the feeding line and resonator, and the spacing between SIRs.

The basic structure of a $\lambda/4$ microstrip SIR is shown in Figure 5. It consists of two segments of lines with different characteristic impedances Z_1 and Z_2 and of electrical lengths θ_1 and θ_2. It's observed that space between the fundamental and spurious frequencies can be controlled by the value of R_Z in this case in [6]. In this study, the

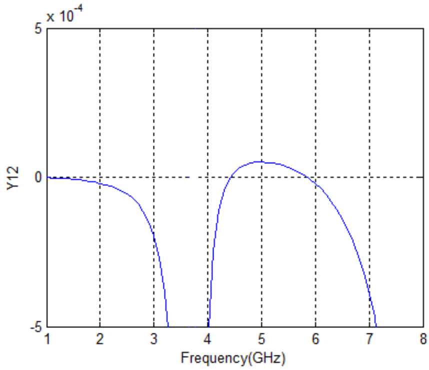

Figure 4. Transmission zeros of the single-band filter.

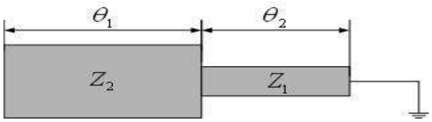

Figure 5. General structure of $\lambda/4$ SIR.

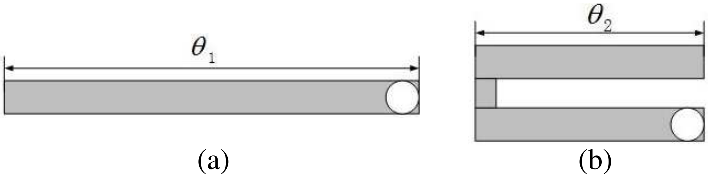

Figure 6. $\lambda/4$ transmission line, (a) the original one, (b) the bent one.

resonator ($\lambda/4$ transmission line) is bended, which not only reduces the size of the filter but can obtain some other characteristics.

As shown in Figure 6, the input impedance of the original resonator can be expressed as

$$Z_{\text{in1}} = jZ_o \tan(\theta_1) \tag{13}$$

The impedance matrix of the remaining two-port may be written as

$$Z_{11} = Z_{22} = j\frac{Z_{oe}}{2}\cot\theta_e + j\frac{Z_{oo}}{2}\tan\theta_o \tag{14}$$

$$Z_{12} = Z_{21} = -j\frac{Z_{oe}}{2}\cot\theta_e - j\frac{Z_{oo}}{2}\tan\theta_o \tag{15}$$

$$Z_{\text{in2}} = Z_{11} + \frac{Z_{12}Z_{21}}{Z_L - Z_{22}} \tag{16}$$

where $Z_L = 0$. Z_{oe} and Z_{oo} are the even and odd mode characteristic impedances, and θ_e and θ_o are the even and odd mode electric lengths for coupled-transmission-line section.

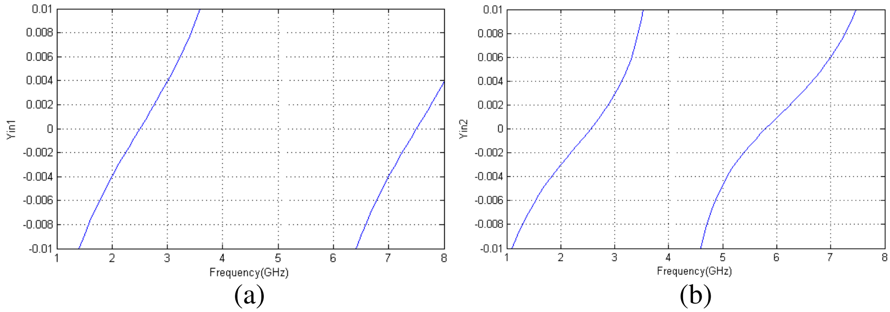

Figure 7. Plot of the characteristic functions of (17) and (18). (a) The characteristic functions of (17), (b) the characteristic functions of (18).

From mechanisms the resonator resonates, its input admittance is set to be zero.

$$Y_{\text{in1}} = \frac{1}{Z_{\text{in1}}} = 0 \tag{17}$$

$$Y_{\text{in2}} = \frac{1}{Z_{\text{in2}}} = 0 \tag{18}$$

By setting the center frequency of the two resonators at 2.4 GHz, we can get from Figure 7 that the second order mode is shifted after being bended.

As shown in Figure 7, the second resonant frequency of the original resonator is at 7.5 GHz but at 5.8 GHz with the bented one. Therefore, the second resonant frequency can be shifted down by bending the transmission line, with smaller ratio of line impedance of SIRs obtained. The smaller ratio of the line impedance can get the required ratio of the resonant frequency of the higher to the resonant frequency for the $\lambda/4$ SIR. This property makes it easy to fabricate since width of a microstrip line of characteristic impedance Z_2 is too narrow to be fabricated only adopting SIR theory.

Considering the two factors mentioned above, the stepped-impedance ratio R_Z is selected as 1.4 for $\theta_1 = \theta_2$.

The output external quality factor Q_{e1} and Q_{eN} can be determined as follows:

$$Q_{e1} = Q_{eN} = \frac{\psi_1}{J_{01}^2/G_A} \tag{19}$$

$$\psi_1 = Y_2 \arctan \sqrt{R_Z} \tag{20}$$

$$\frac{Z_{oo}}{Z_o} = \frac{1 - J_{01} Z_o \csc\theta_c + J_{01}^2 Z_O^2}{1 - J_{01}^2 Z_o^2 \cot\theta_c^2} \tag{21}$$

$$\frac{Z_{oe}}{Z_o} = \frac{1 + J_{01} Z_O \csc\theta_c + J_{01}^2 Z_O^2}{1 - J_{01}^2 Z_o^2 \cot\theta_c^2} \tag{22}$$

where ψ_1 is the susceptance slope parameter; J_{01} is the admittance inverter parameter between feeding line and the resonator; R_Z is the ratio of the impedance; Y_2 is the admittance of line in Figure 5. Z_{oe} and Z_{oo} are the even and odd mode characteristic impedances for coupled-transmission-line section; θ_c is the electric length.

The space 'S' between feeding line and SIR can be obtained from Z_{OO} and Z_{Oe}. Coupling coefficients with the spacing between adjacent SIRs can be obtained in Figure 8, in which $\varepsilon_\gamma = 2.55$, loss tangent $\delta = 0.0029$, and thickness $h = 0.8$ mm. Thus, the spacing are selected as $s = 0.2$ mm, $s1 = 1.3$ mm.

The schematic of the proposed bended SIRs filter is shown in Figure 9(a) and the frequency response is shown in Figure 10(a). From Figure 10(a) that the third transmission zero shifts downward when the uniform impedance resonator (UIR) changes to SIR.

To validate the diversity of the filter configuration, another bended configuration of the SIRs dual-band passband filter is shown in Figure 9(b). And the simulated frequency responses of the two configurations are shown in Figure 10. As shown in Figure 10, both the filters have the same and good performance. The overall areas of the two models are 12 mm $*$ 12 mm and 9 mm $*$ 14 mm respectively.

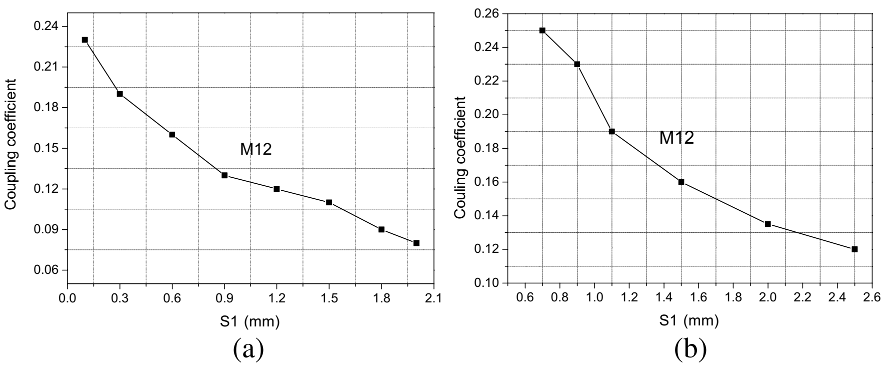

Figure 8. Coupling coefficients of the dual-band filter at different frequencies. (a) $f_0 = 2.4$ GHz, (b) $f_0 = 5.2$ GHz.

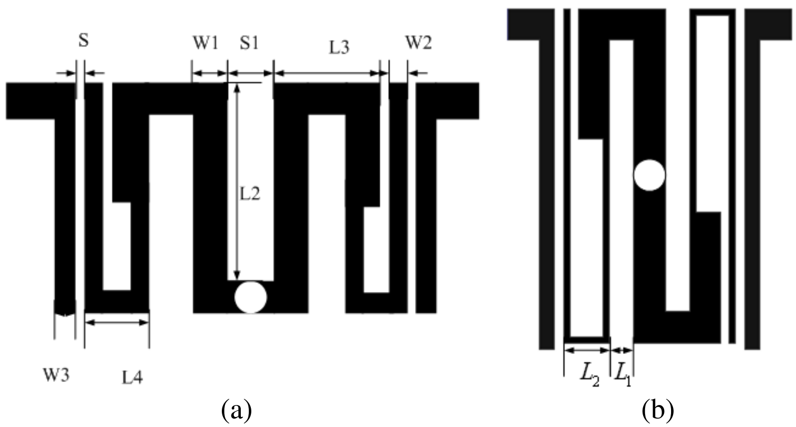

Figure 9. Configurations of the SIR dual-band passband filter.

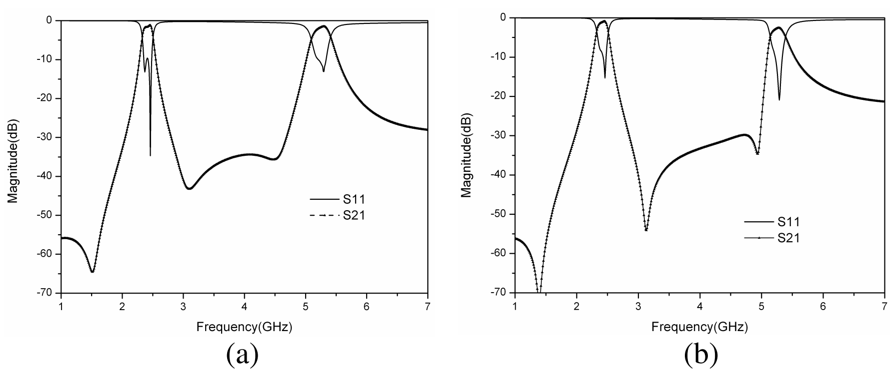

Figure 10. Simulated frequency responses of the two filters. (a) Frequency response of Figure 9(a), (b) frequency response of Figure 9(b).

4. SIMULATED AND MEASURED RESULTS

A sample BPF (Figure 9(a)) circuit design using the above method was fabricated and measured using Network Analyzer for performance demonstration. The main physical dimensions of the filter in Figure 9(a) are denoted as follows: $W_1 = 1\,\text{m}$, $W_2 = 0.5\,\text{mm}$, $W_3 = 0.5\,\text{mm}$, $S_1 = 1.2\,\text{mm}$, $L_2 = 8\,\text{mm}$, $L_3 = 2.8\,\text{mm}$, $L_4 = 1.8\,\text{mm}$, $L_5 = 4.5\,\text{mm}$, $S = 0.2\,\text{mm}$. The filter is etched on a substrate with dielectric constant $\varepsilon_\gamma = 2.55$, loss tangent $\delta = 0.0029$, and thickness $h = 0.8\,\text{mm}$.

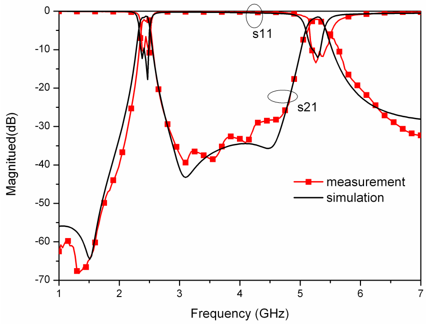

Figure 11. Simulated and measured results of the proposed dual-band filter.

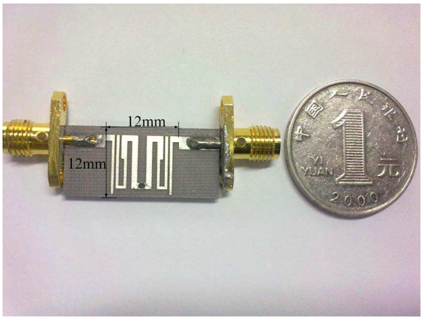

Figure 12. Photograph of the fabricated filter.

The simulated and measured responses are shown in Figure 11. It is seen that the measured and simulated performance are in good agreement. As shown in Figure 11, the passbands exist at 2.4 GHz and 5.2 GHz and the relative 3-dB bandwidths are 8.1% and 9.6%. The filter with first resonant frequency at 2.4 GHz has less than 1.8 dB insertion loss and greater than 12 dB return loss. The second resonant frequency at 5.2 GHz has less than 2.1 dB insertion loss and greater than 15 dB return loss. In addition, three transmission zeros are generated in both low and high stopband and a good rolloff is demonstrated in the stopband. Two transmission zeros are at 1.5 GHz and 3.1 GHz on both sides of the passband. The third transmission zeros at 4.8 GHz is observed. The suppression on both sides of 2.4 GHz is greater than 45 dB, and the filter at 5.2 GHz reaches 30-dB suppression, a high out-of-band rejection obtained.

Figure 12 shows a photograph of the proposed filter, and the overall area is about 12 mm $*$ 12 mm.

5. CONCLUSION

In this paper, a simple and effective method for designing a dual-band filter is proposed, and a sample filter is fabricated. Dual-band responses is generated by adjusting the impedance ratio of SIRs and the bent structure. The existence of transmission zeros is proved, which improves the band selectivity. A design procedure is given for the filter design, and two filters are implemented. The characteristics of the dual-band filter are studied, and the advantages, such as compact size, sharp rolloff, simple and flexible structure, are demonstrated through simulation and experiment. The circuit size is reduced about 50%, and the design is easy to carry out compared with the filter in [11] and [12] with the similar specifications.

REFERENCES

1. Miyake, H., S. Kitazawa, T. Ishizaki, T. Yamada, and Y. Nagatomi, "A miniaturized monolithic dual band filter using ceramic lamination technique for dual mode portable telephones," *IEEE MTT-S Int. Microwave Symposium Dig.*, Vol. 2, 789–792, 1997.
2. Chen, C.-Y. and C.-Y. Hsu, "A simple and effective method for microstrip dual-band filters design," *IEEE Microw. Wireless Compon. Lett.*, Vol. 16, No. 3, 246–248, May 2006.
3. Tsai, L.-C. and C.-W. Hsue, "Dual-band bandpass filters using equal length coupled-serial-shunted lines and Z-transform techniques," *IEEE Trans. on Microw. Theory and Tech.*, Vol. 52, 1111–1117, 2004.
4. Matthaei, G., L. Young, and E. T. Jones, *Microwave Filters, Impedance-Matching Network, and Coupling Structure*, Artech House, Norwood, MA, 1980
5. Chen, Y.-M., S.-F. Chang, C.-C. Chang, and T.-J. Hung, "Design of stepped-impedance combline bandpass filters with symmetric insertion-loss response and wide stopband range," *IEEE Trans. on Microw. Theory and Tech.*, Vol. 55, 2191–2199, 2007.
6. Wu, H.-W., Y.-K. Su, M.-H. Weng, and R.-Y. Yang, "Design of dual-band bandpass filter using diverse quarter-wavelength resonators for GPS/WLAN applications," *Microw. Opt. Technol.*, Vol. 50, No. 10, 2694–2696, Oct. 2008.
7. Deng, H.-W., Y.-J. Zhao, X.-S. Zhang, W. Chen, and J.-K. Wang, "Compact and high selectivity dual-band dual mode microstrip BPF with single stepped-impedance resonator," *Electron. Lett.*, Vol. 47, No. 5, 326–327, Mar. 2011.
8. Wu, Y.-L., C. Liao, and X.-Z. Xiong, "A dual-wideband bandpass filter based on eshaped microstrip SIR with improved upper-stopband performace," *Progress In Electromagnetics Research*, Vol. 108, 141–153, 2010.
9. Xue, W., C.-H. Liang, X.-W. Dai, and J.-W. Fan, "Design of miniature planar dual-band filter with 0° feed structures," *Progress In Electromagnetics Research*, Vol. 77, 493–499, 2007.
10. Chen, C.-Y. and C.-C. Lin, "The design and fabrication of a

highly compact microstrip dual-band bandpass filter," *Progress In Electromagnetics Research*, Vol. 112, 299–307, 2011.

11. Yang, R.-Y., "Design of dual-band bandpass filters using a dual feeding structure and embedded uniform impedance resonators," *Progress In Electromagnetics Research*, Vol. 105, 93–102, 2010.
12. Ma, D., Z. Y. Xiang, X. Wu, C. Huang, and X. Kou, "Compact dual-band bandpass filter using folded SIR with two stubs for WLAN," *Progress In Electromagnetics Research*, Vol. 117, 347–364, 2011.
13. Chang, Y.-C., C.-H. Kao, M.-H. Weng, and R.-Y. Yang, "A novel compact dual-band bandpass filter using asymmetric SIRs for WLANs," *Microw. Opt. Technol. Lett.*, Vol. 50, No. 8, 1237–1240, May 2008.